Chapter-1

Introduction and Literature Review

CHAPTER 1: Introduction and Literature Survey

1.1 Present Energy Scenario

Energy is a necessary component of our everyday existence, and its accessibility is crucial for the advancement of the economy and society. Nevertheless, the global community is currently confronted with an energy crisis as a result of a combination of factors, including population growth, increased industrialisation, and urbanisation. Global energy consumption and demand are experiencing tremendous growth in recent times. It is projected that electricity demand would rise by about 30 terawatts by 2050 (Figure 1.1). Therefore, we require a source of energy that is less harmful to the environment, more economically viable, and more efficient in terms of energy use [1]. Subsequently, numerous research initiatives are being implemented to establish an efficient power generation system.

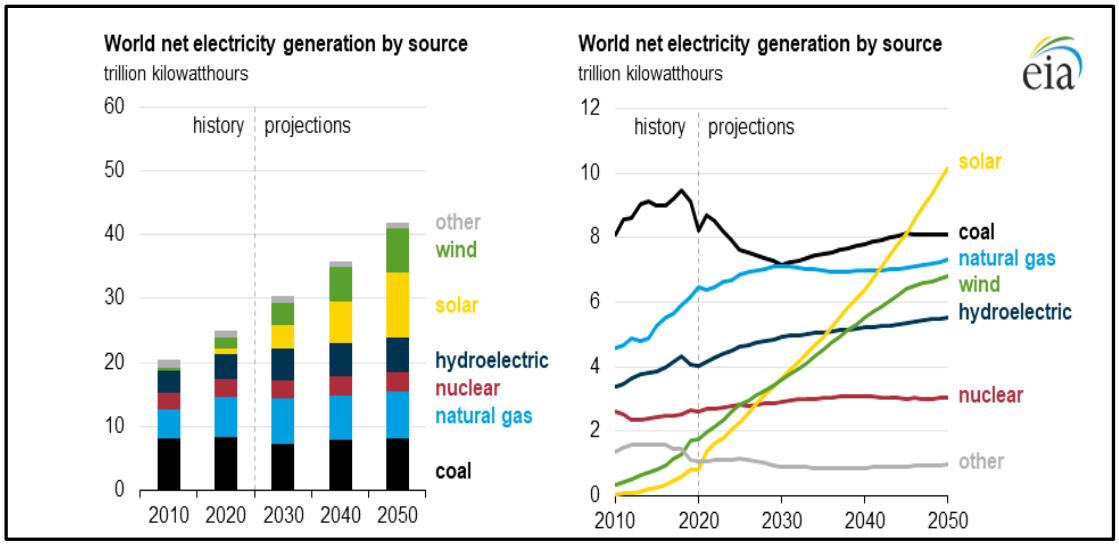

Figure 1.1 Energy production from 2010 to 2050 using various energy sources [2].

1.1.1 Global Energy Crisis

The energy crisis is a complex issue caused by an imbalance between energy supply and demand.This crisis is caused by geopolitical conflicts, economic instability, environmental concerns, and uneven resource distribution. The effects of an energy crisis would go well beyond a general economic slump because of how much the globe depends on energy for progress and survival. It has an impact on the sustainability of the environment, as well as social and international relations conditions.

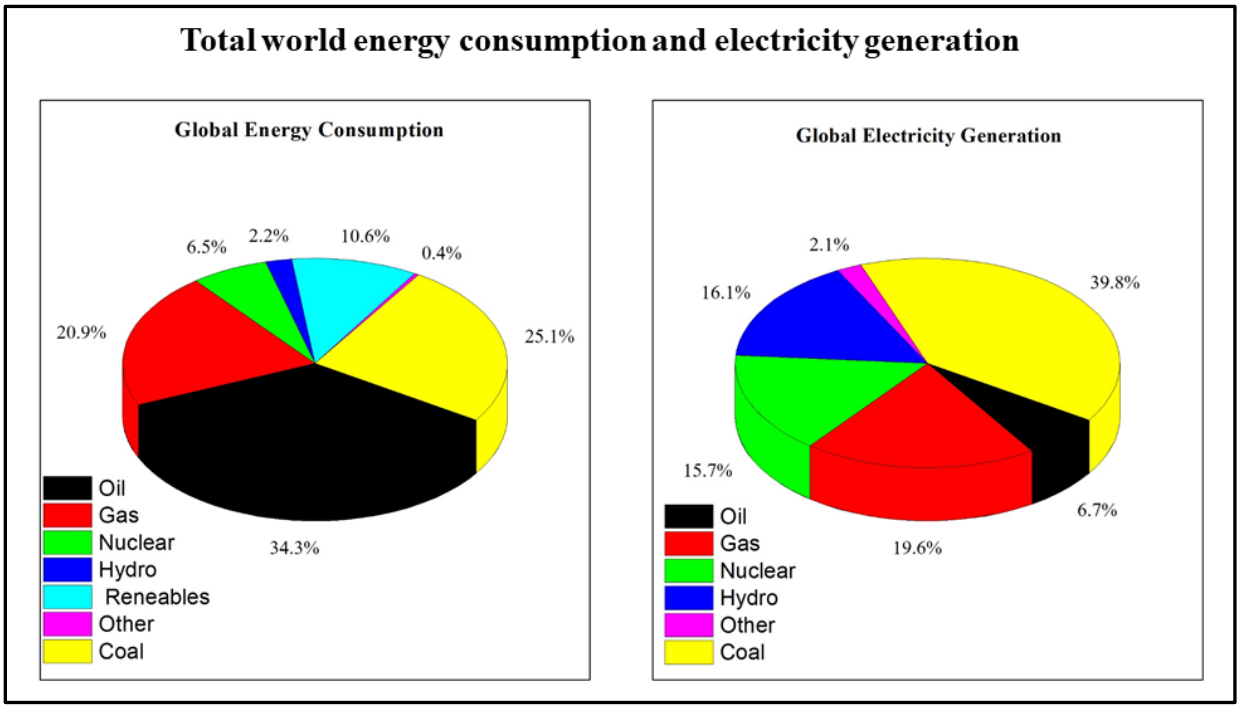

Figure 1.2 Energy consumption and electricity generation over the previous year [3].

Since energy is considered one of the most important drivers of economic growth in all economies [4], research on the critical role energy plays in the process of economic development as well as the relationship between energy consumption and economic growth has increased [5].

These factors, both individually and collectively, contribute to the complex and multifaceted nature of the global energy crisis (Figure 1.3).

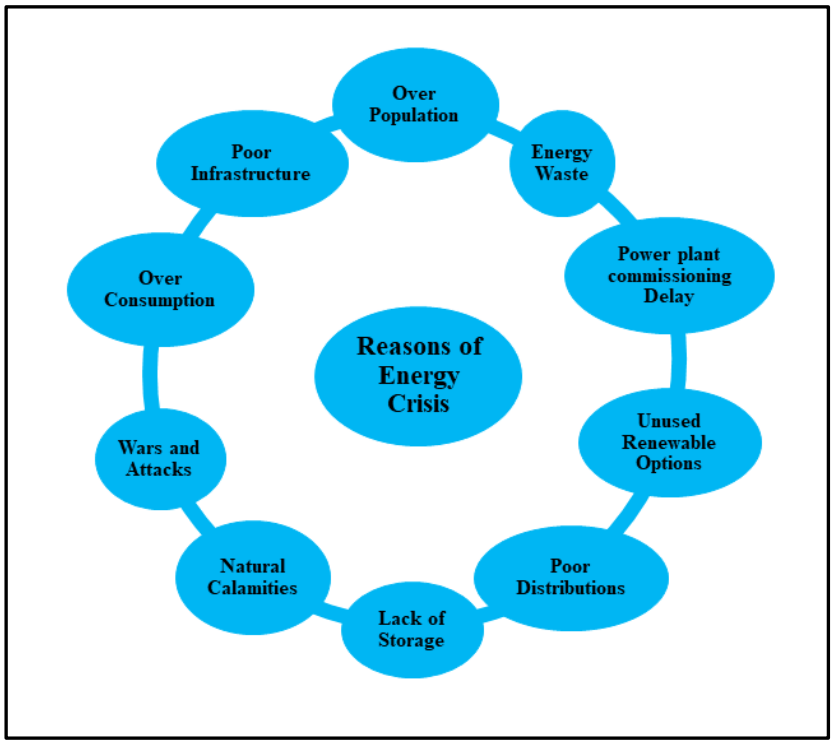

Figure 1.3 Reasons of energy crisis

1.1.2 Possible Solutions of energy crisis:

Renewable energy is a prominent and significant alternative energy source. Renewable energy sources are non-depletable, sustainable, environmentally beneficial, and safer for human health[6]. Because of the enormous environmental benefits, research into the creation of renewable energy systems from various sources has grown in recent years. Hydro, solar, and wind power can protect against an energy catastrophe since fossil fuels cannot meet rising electricity demand [7]. There is ther various renewable energy sources are present on the earth

like wind energy, solar energy, hydro-electricity, geothermal energy and biomass energy (Figure1.4)

Figure 1.4 Different renewable energy sources

1.1.3 Solar Energy- An Alternative Option

Among all the alternative energy sources that are now available solar energy is a highly suitable renewable alternative for tackling the energy problem because of its abundant availability, sustainability over the long term, and minimal environmental impact. The technology utilises solar energy, an inexhaustible global resource, hence decreasing reliance on limited fossil fuels [8]. Due to technological advancements, solar electricity has become efficient and cost-effective, enabling its wider accessibility [9]. Solar panels can be installed in a variety of locations, including rooftops and open fields, and require minimal maintenance once they are installed [10]. Solar energy also decreases the release of greenhouse gases, which aids in the fight against climate change.Furthermore, it promotes energy self-sufficiency by allowing for local electricity production, thereby supporting a cleaner and more reliable future [8]. India's economy is growing rapidly, so there will be a significant rise in energy consumption as

well[11]. The government of India has set an ambitious target of installing 175 Gigawatt (GW) renewable energy capacity by 2022, which included solar power (100 GW) wind power (60 GW) and bio-gas & small hydropower (15GW) [12][13].

Solar energy is distributed in three major bands or regions of solar spectrum , Ultraviolet, Visible and Infrared. The radiant energy that reaches the Earth is composed of roughly 42.9% visible light, 49.4% infrared radiation, and about 8% ultraviolet radiation of the total energy[14]. Approximately 29 percentage of the solar energy that reaches the Earth's atmosphere is redirected back into space by various factors such as clouds, air particles, and reflective surfaces like sea ice and snow. This energy does not have any impact on Earth's climate system, 48% of the solar energy that enters the atmosphere is absorbed by the surface, while the remaining 23% is absorbed by dust, ozone, and water vapor in the atmosphere. As a result, the Earth system absorbs roughly 71% of all solar energy that is directed towards it[15][16].

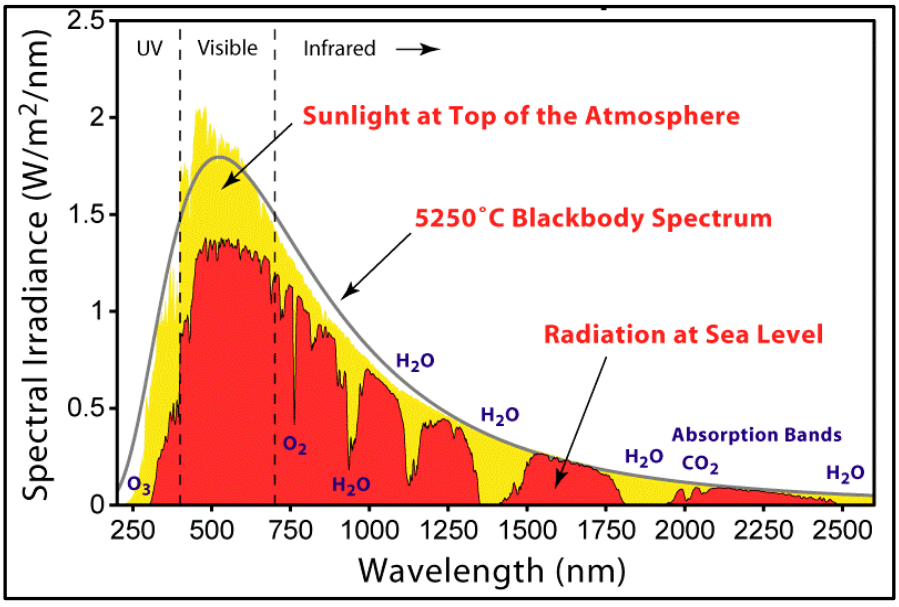

Figure 1.5 Illustrates the spectrum of solar radiation [17].

The photosphere of the Sun, with a temperature of approximately 5800 K, serves as the main source of solar radiation. The spectrum has resemblance to that of a black body radiator with the identical temperature [18]. In order to achieve success, solar energy must effectively capture a wide range of energy that correspond to the solar spectrum (Figure 1.5)

Solar irradiance refers to the amount of radiation that reaches the Earth's atmosphere and is quantified in terms of watts per square meter (W/m^2). The solar irradiance at a specific place or body of water is influenced by factors such as the altitude above sea level, the angle of the sun (determined by latitude, season, and time of day), and scattering components like clouds. The solar irradiance is determined by the angle of the sun. As the angle increases, the solar intensity decreases shown in figure 1.6 [19].

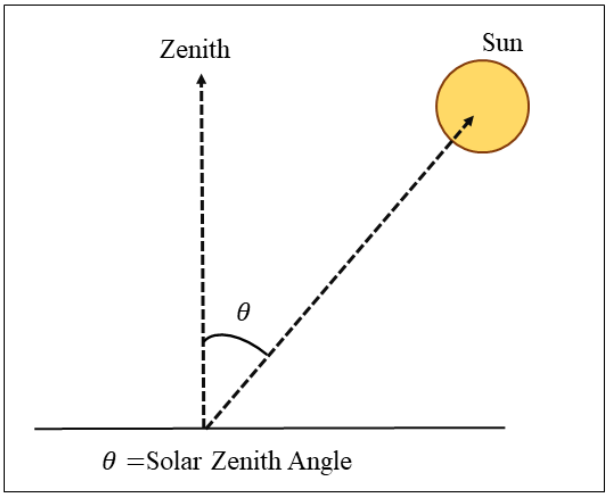

Figure 1.6 The sun's angle determines solar irradiation

The Earth's surface absorbs sunlight across a wide range of wavelengths, spanning ultraviolet to infrared.

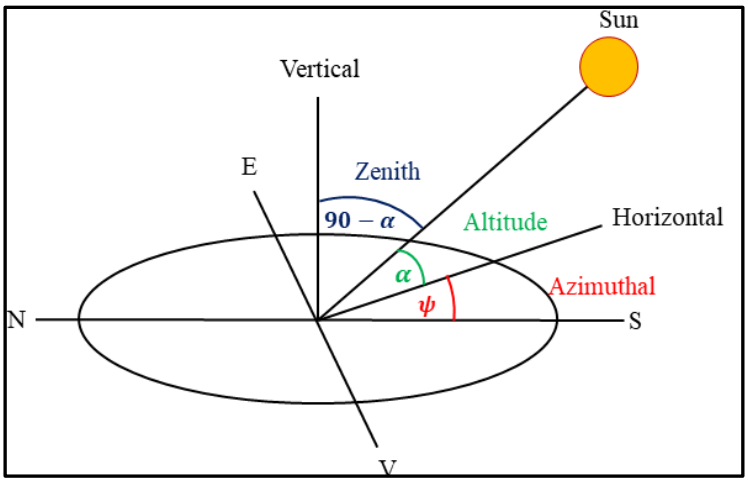

Figure 1.7 Angles describing the sun's position in the sky [14].

The intensity of radiation is determined by the position of the Sun in the sky, which is continually changing as a result of the Earth's rotation on its axis and its orbit around the Sun. At a given point of time, it can be defined by three angles, angle of elevation, azimuthal angle and angle of inclination as shown in the figure1.7[13] An air mass refers to the distance that solar radiation travels and is closely connected to its degree of absorption [20]. It may be calculated using the formula $AM = 1/cos\theta$, where θ represents the angle between the sun and the vertical axis (figure 1.8). The Air Mass (AM) 1.5G is a standardized representation of the spectrum irradiation, characterized by an integrated power density of 1000 W/m^2 and an angle of incidence (θ) of 45 degree [21]. Utilizing photovoltaic (PV) solar cells for power generation shows great potential in turning sunlight into electrical energy. Therefore, solar energy, a sustainable and environmentally friendly energy source, has the potential to provide significant benefits to the economy and climate of both developed and developing countries in the future[22].

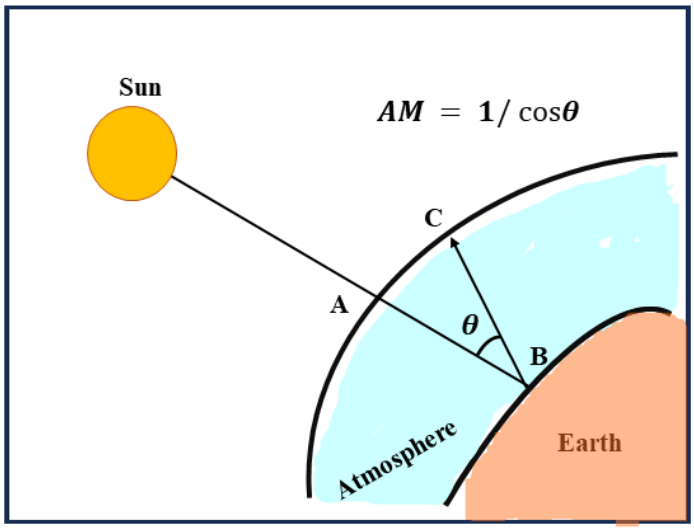

Figure 1.8 Determination of the Air Mass Index [23].

1.2 Working Principle of Solar Cell

A phenomena known as photovoltaics is the process by which sunlight is converted into electricity via the use of semiconductor materials. This effect is referred to as the photovoltaic effect[24]. The photovoltaic effect was initially discovered by *Edmund Becquerel* in 1839. He made the observation that an electric current was produced when light was allowed to shine on a platinum (Pt) electrode that had been coated with silver (Ag) and was submerged in electrolyte[25].

A photovoltaic solar cell is made up of three main parts. Firstly, there is the light absorber, also known as the active layer, which is responsible for transforming incoming photons into electrons and holes. The second component is the carrier collectors, which are responsible for collecting the electrons and holes, and the third component is the metal contacts, which are responsible for transmitting the electrons and holes inside the circuit.

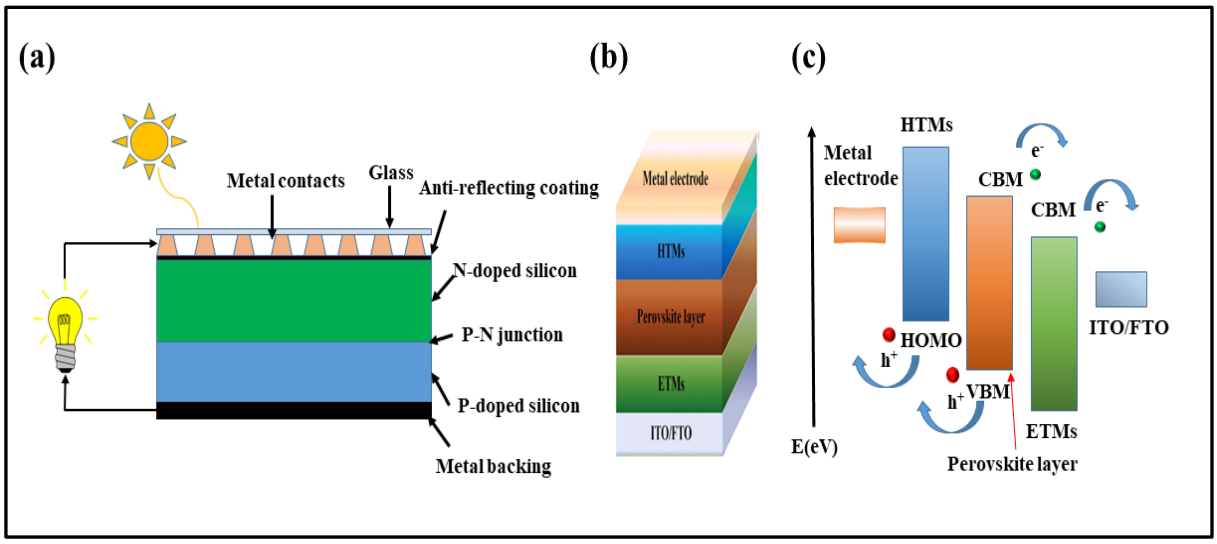

Figure 1.9 (a) shows the fundamental components of a solar cell[21] (b) symbolises architect of perovskite solar cell (c) The operational mechanism of a perovskite solar cell [26].

Figure 1.9(b) depicts the architecture of solar cells with various layers. The perovskite layer, also known as the active layer, produces electrons and holes by absorbing photons from sunshine. These two processes occur simultaneously, with photogenerated electrons moving towards the cathode via the electron transport layer (ETL) and holes moving towards the anode via the hole transport layer. The purpose of ETL (electron transport layer) and HTL (hole transport layer) is to gather charge carriers created by light and facilitate their transport to the appropriate electrodes [27]. The very first solar cell design, also known as the PN junction and utilising amorphous Silicon semiconductor, was developed at Bell Laboratories in 1954. It achieved an efficiency of 6% and quickly gained significant interest [28]. Silicon-based solar cells now dominate the photovoltaic (PV) market due to its ability to achieve high efficiency of around 26%, while also having relatively modest fabrication costs. Additionally, thin-film technologies that are based on III-V semiconductors demonstrated good efficiencies. Over the course of the last twenty years, a number of solar technologies of the next generation have been developed.It consists of QD solar cells, DSSCs, organic photovoltaics, etc[29][30].

1.3 Characteristics of Solar Cells

The performance of solar cells can be determined by analysing the specific characteristics acquired from the I-V curve, which represents the behaviour of solar cells under sunlight exposure. There are a number of important metrics to consider, such as the following: fill factor (FF), maximum power output (P_{max}), power conversion efficiency (PCE), open-circuit voltage (V_{OC}), and short circuit current (I_{sc}). Figure 1.10 depicts the schematic representation of the equivalent circuit model for a solar cell. In an ideal scenario, the shunt resistance (R_{sh}) of a solar cell would be infinite, while the series resistance (R_s) would be zero. The variables I_D, I_L, and I_{SH} correspond to the voltage-dependent current that is dissipated by recombination, the current created by light in the cell, and the current that is lost due to the shunt resistance, respectively [31].

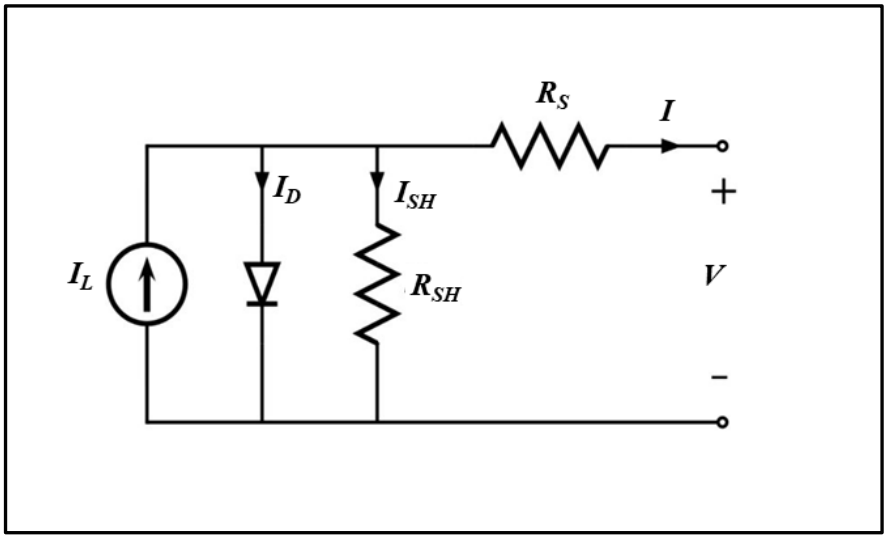

Figure 1.10 Equivalent circuit model of the solar cell[32].

1.3.1 The current-voltage (I-V) characteristics

Solar cells with p-n junctions, such as diodes, exhibit nonlinear current-voltage (I-V) characteristics. An perfect solar cell exhibits a current-voltage curve that is located in the fourth quadrant. As the solar cell starts to produce electricity when light hits it, the I-V curve moves into the fourth quadrant; the magnitude of this shift is proportional to the intensity of the light hitting the cell. The equation representing the relationship between current and voltage in the fourth quadrant is:

$$I = I_L - I_0 \left[\exp\left(\frac{qV}{\eta kT}\right) - 1\right] \quad (1.1)$$

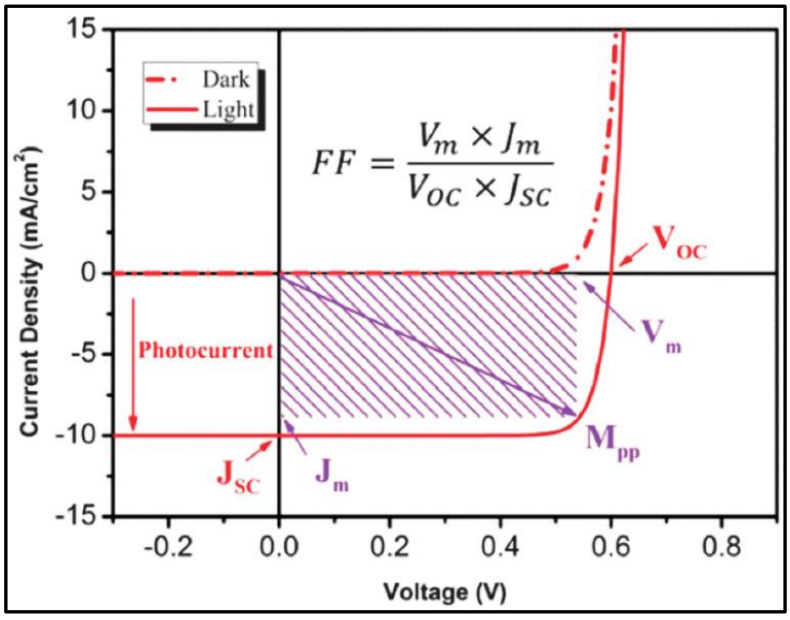

Figure 1.11 Schematic representation of the I-V characteristics of a solar cell in both dark and light conditions[33].

The variables I_0, I_L, V, and q corresponds to the reverse saturation current of the diode, the photo-generated current of the diode, voltage that is applied, and the basic charge, respectively.

Moreover, the diode's ideality factor, temperature, and Boltzmann constant are represented by the symbols κ, T and η respectively [34].

1.3.2 Open-Circuit Voltage (V_{oc})

The V_{oc} is derived from the potential difference resulting from the intrinsic electric fields (E_{in}) of the n- and p-type regions. The highest voltage that can be produced between a solar cell's terminals while it is not connected to any external circuit is known as the open-circuit voltage. That means, the current is equal to zero (I=0) .The voltage measured when there is no current flowing in a circuit can be observed on the current-voltage curve shown above. The equation for open-circuit voltage V_{oc} is obtained by putting the value of current (I=0) into the aforementioned solar cell equation

$$V_{oc} = [\frac{nkT}{q} ln(\frac{I_L}{I_0} + 1)] \quad (1.2)$$

The solar cell's open-circuit voltage(V_{oc})is based on its saturation current (I_0)and the current produced by light (I_L). Although the I_{sc} typically shows minimal variance, the primary factor that might significantly shift is I_0, which may vary by a factor of ten. The value of I_0 is depend upon the recombination process occurring within the solar cell. Hence, the level of recombination in the device is quantified by the open-circuit voltage V_{oc}. In addition, the geometry of the active layer material influences V_{oc}, which requires a more favourable alignment between the metal electrode and the semiconductor (deposited active layer) [35].

1.3.3 Short-Curcuit Current (I_{sc})

The term "short-circuit current," which is often referred to as "short-circuit photocurrent," describes the electric current that flows through a solar cell when the voltage that is provided

to the cell is significantly lower than itself. Essentially, when a solar cell is short-circuited, the current flowing through the solar cell is of a negative magnitude. A solar cell's maximum short-circuit current is influenced by a number of factors, such as the device's size, light intensity, incident light's spectral distribution, and surface absorption or reflection. Maximising the amount of electrons and holes that migrate to each electrode is required to provide a large short-circuit current (I_{sc}), while avoiding the recombination of photogenerated electrons and holes and their reflection on the solar cell's surface[36]. The formula for determining the short circuit current in an ideal cell with consistent generation and a non-active surface is as follows:

$$I_{sc} = qAG(L_n + L_p) \quad (1.3)$$

G, *A*, L_n, and L_p represent the rate of generation of charge carriers, surface area of the solar cell, and the diffusion length of charge carriers, respectively. The term "I_{sc}" indicates the direct correlation between the diffusion length and the rate of generation of charge carriers.

1.3.4 Maximum Power Output (P_{max})

A solar cell's maximum power output is the highest amount of power it can produce. The maximum power output refers to the highest level of electricity that a solar cell can generate. The equation can be expressed as $P_{max} = I_m V_m$, where V_m denotes the maximum voltage and the I_m denotes the maximum current. This behaviour can be observed in the fourth quadrant of the current-voltage curve (Figure 1.11). Within the context of solar cells, the term "operating point" refers to the precise moment at which the amount of electricity that is delivered reaches its maximum value. The highest amount of power that a solar cell can deliver is known as its power output.

1.3.5 Fill Factor (*FF*)

The term "FF" refers to the productivity of a device in generating carriers through the absorption of light within the solar cell. Theoretical FF is almost 100%, which closely aligns with the rectangular shape depicted in the I-V curve (Figure 1.8). The maximum fill factor (FF) in the solar cells that have been recorded is limited to 90%. The fill factor numbers are usually between 0.7 and 0.8 because of some problems with the way the cells are designed. In addition to this, the fill factor is dependent on temperature, and it reduces as the temperature rises. The decrease in the fill factor (FF) is mainly governed by a decrease in the open-circuit voltage (V_{oc}), whereas the rise in the short-circuit current (I_{sc}) due to temperature does not significantly contribute to the fill factor. The power of the incident light on the device is what determines the expression of fill factor (FF) [37][38]. FF is expressed as follows:

$$FF = \frac{V_m I_m}{V_{oc} I_{sc}} = \frac{P_{max}}{V_{oc} I_{sc}} \quad (1.4)$$

where I_m represents the current at maximum power and V_m represents the voltage at maximum power.

1.3.6 Power Conversion Efficiency (*PCE*)

The power conversion efficiency (PCE) of a solar cell is an essential factor in determining the conversion efficiency of the cell.The efficiency of solar cells is measured by the ratio of the amount of energy they produce to the amount of energy they receive from the sun. The power conversion efficiency, which is computed based on the standard dark and illumination circumstances (AM 1.5: 100 mW/cm² at 25 ℃),offers the electrical producing parameters that are used to evaluate the effectiveness of solar cells[33].

$$\eta = \frac{V_m I_m}{P_{in}} \times 100\% \quad (1.5)$$

Efficiency is connected to I_{sc} and V_{oc} using FF as given by,

$$\eta = \frac{V_{oc} I_{sc}}{P_{in}} \times FF \quad (1.6)$$

Moreover, the performance of the solar cell is influenced by the temperature, spectrum, and intensity of the incident sunlight. In light of this, it is imperative that the conditions under which efficiency is evaluated for the purpose of performance comparison be meticulously monitored [39].

1.4 Generations of Solar Cell

There are three generations of photovoltaic technologies: the first, the second, and the third generation. These generations are distinguished from one another by the primary materials that are utilised and the degree of commercial maturity that the technology has reached [40].

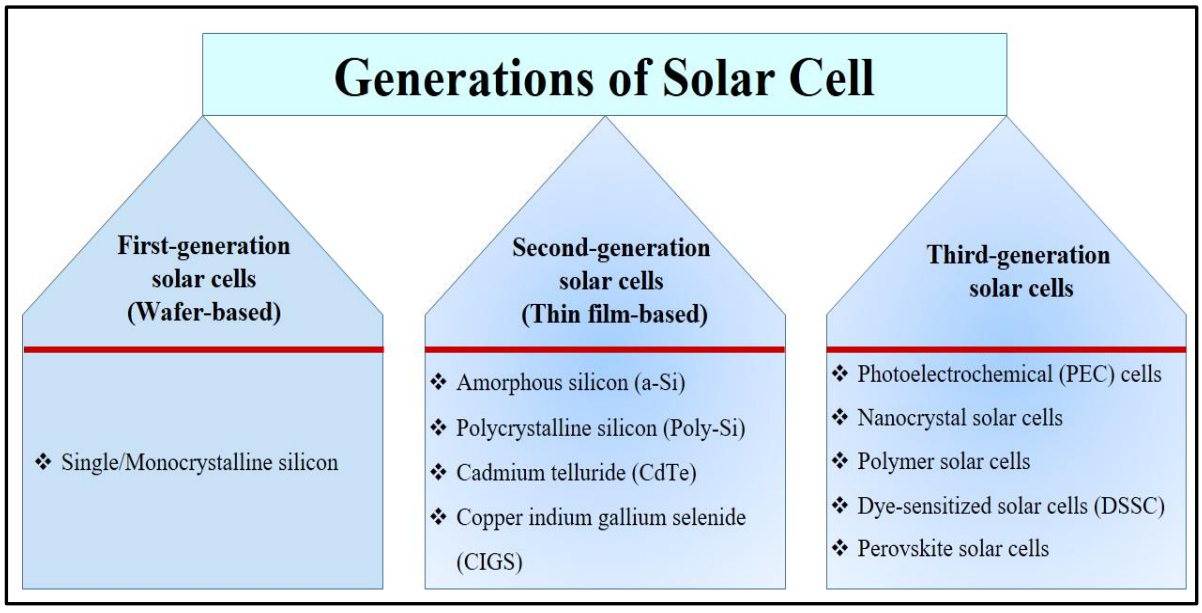

Figure 1.12 Generations of the Solar Cell[41].

1.4.1 First generation solar cells

The first generation of solar cells comprises of single-junction cells that use wafers made of either monocrystalline or polycrystalline silicon PV technology. Silicon is the most popular material used in PV modules due to its remarkable mechanical, chemical, and electrical qualities[42]. This semiconductor is the foundation upon which solar technologies are considered to be the most cutting-edge.Generally, Czochralski (CZ) technique is used to fabricate silicon wafers.

Table 1.1 1st generation photovoltaic cells

Type	Efficiency	Advantages	Disadvantages
Mono-crystalline silicon	• Laboratory efficiency ranges from 25–27%, making it the most efficient among all solartechnologies[43]. • The commercial efficiency falls somewhere in the region of 16–22%. • The band gap is between 1.11 and 1.15 electron volts (eV).	This particular solar panel is characterised by its exceptional purity and remarkable efficiency.	The manufacturing process, particularly the CZ approach, involves a substantial amount of materials and energy.
Polyc-rystalline silicon	• 15–18% • The band gap is1.11eV[44].	An effective solution to reduce the cost of photovoltaic (PV) modules.	a lower efficiency compared to mono crystalline-Si cells

1.4.2 Second generation solar cells

The second-generation solar cells utilise thin-film photovoltaic (PV) devices built from amorphous silicon, copper indium gallium selenide (CIGS) and cadmium telluride (CdTe). The

thickness of film layers can vary from a few nanometres (nm) to tens of micrometres (μm). The primary benefit of this technology is its low cost of production and materials because each cell requires a relatively small amount of semiconductor material.

Table 1.2 2nd generation photovoltaic cells.

Type	Efficiency	Advantages	Disadvantages
Amorphous Silicon(a-Si)	• Modules on the market typically have a 4-8 % efficiency. • Laboratory small cells can achieve a 12 % efficiency[44].	Solar cells made on amorphous silicon are the most economical choice.	In comparison to single-crystalline silicon (sc-Si) and multi-crystalline silicon (mc-Si), the layers are considerably thinner and have a lower amount of material to capture solar energy.
Gallium Arsenide (GaAs)	• According to the recorded laboratory efficiency, 29 % [46]. The band gap measures 1.43 eV.	In comparison to silicon, it is more efficient and has a smaller thickness.	High manufacturing cost.
Cadmium Telluride (CdTe)	• Recorded efficiency between 10-15%[46]. • The band gap is 1.45 eV.	Cadmium telluride (CdTe) cells have the ability to utilise a wider range of wavelengths compared to silicon (Si) cells, which is nearer to the natural spectrum.	Pure cadmium is known to be one of the most poisonous elements, and cadmium telluride has some of the same dangerous characteristics..
Copper Indium Gallium Selenide (CIGS)	• 20% (subject to specific conditions) • The band gap is 1.68 (eV).	• Process consumes less energy than crystalline silicon solar cell production. • Exceptional resilience to excessive heat	• This particular solar cell exhibits lower efficiency compared to silicon-based solar cells. • At present, the cost of production is too high.

1.4.3 Third generation solar cells

The third generation of solar panels incorporates a wide range of innovative technologies, the majority of which are currently in the research and development stage.

Table 1.3 3rd generation photovoltaic cells.

Type	Efficiency	Advantages	Disadvantages
Perovskite solar cell (PSC)	Approximately 19 to 22% [46].	• High efficiency and significant potential for enhancement. • When compared to silicon, perovskite has a lower production cost.	• Perovskite undergoes rapid degradation when subjected to heat, precipitation, moisture, and other environmental factors.
OPV and polymer solar cells	The range is 4-5%, with a maximum of 9%[46].	In addition to being lightweight, mechanically flexible, disposable, and having large-scale applications, it also has these features.	Low efficiency, durability, and instability.
Dye-sensitized solar cell (DSSC)	Around 10%.	• Flexible, non-polluting, and readily recyclable. Cost-effective due to the simplified manufacturing process.	The electrolyte has the potential to freeze at low temperatures, which might result in a decrease in power generation and cause damage to the body.

The third-generation photovoltaic (PV) technology encompasses various types of solar systems, including dye-sensitized solar cells (DSSC), organic solar cells, quantum dot cells, polymer solar cells, and perovskite solar systems.

1.5 Perovskite Crystal Structure, and Goldschmidt Tolerance Factor

Perovskite has a crystal structure that is identical to that of the mineral calcium titanium oxide ($CaTiO_3$). Gustav Rose made the discovery of this mineral in the Ural Mountains of Russia in the year 1839.This crystal structure is shared by all materials with the ABX_3 universal chemical formula. In this formula, 'X' stands for an anion while 'B' and 'A' are cations with varying ionic radii; the 'B' atoms are smaller than the 'A' atoms. The ideal perovskite structure, abbreviated as ABX_3, consists of a cubic cell with a 'B' cation in 6-fold coordination, surrounding by an octahedron of anions (X), and an A cation in 12-fold cuboctahedral coordination in one corner of the cell (Figure 1.13)[47]. The X anion for halide-based perovskites can be either Iodine (I), Bromine (Br), or Chlorine (Cl). The B cation can be Lead (Pb^{2+}), or Tin (Sn^{2+}), while the A cations can be Caesium (Cs^{+}), Copper (Cu^{+}), FA (formamidinium $NH_2CH{=}NH_3^{+}$), MA^{+} (methylammonium,$CH_3NH_3^{+}$),or Rubidium (Rb^{+})[48]. The relative ion size has a significant impact on the stability of the perovskite cubic structure. Consequently, the structure can be deformed as a result of even a minor change in the ion size. The Goldschmidt tolerance factor was developed by Victor G. Goldschmidt as a powerful instrument for assessing the durability of crystal structures and distortions.

The Goldschmidt tolerance factor, denoted as τ, is described by the following equation:

$$\tau = \frac{(r_A + r_X)}{\sqrt{2}(r_B + r_X)} \qquad (1.7)$$

The ionic radii of cation A, cation B, and anion X are denoted by the symbols r_A, r_B, and r_X respectively. The tolerance factor is 1 for an ideal cubic perovskite structure. Another way to vary the tolerance factor is to change the ionic radius of the ions.

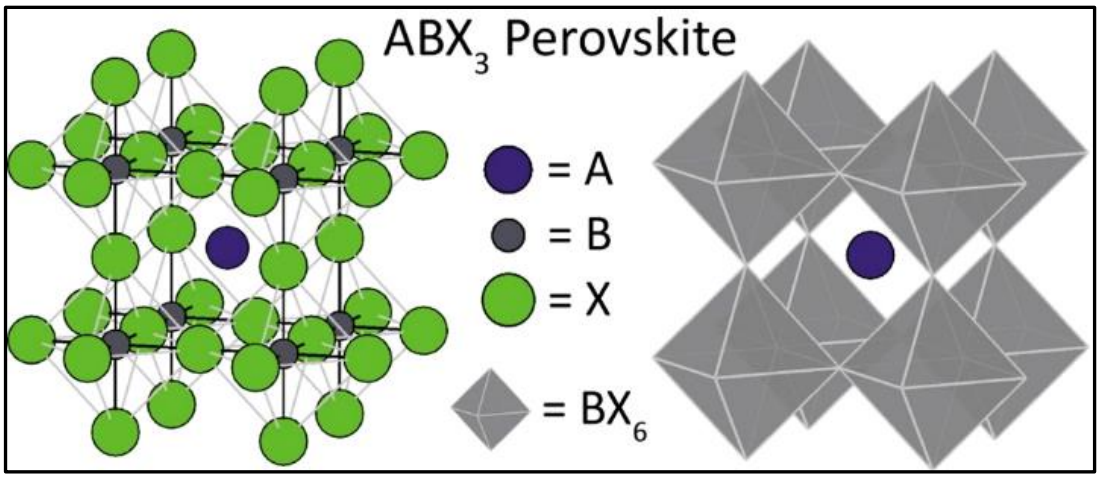

Figure 1.13 Arrangement of atoms in the perovskite substance [49].

The ratio of μ = r_B/r_X represents the octahedral factor. In order to achieve a stable halide perovskite, the values τ and μ should fall within the range of $0.81 < \tau < 1.11$ and $0.44 < \mu < 0.90$ [49]. In cases where the value of τ is lower, the perovskite exhibits less symmetry, such as tetragonal or orthorhombic shape. When $\tau > 1$, the 3D (three-dimensional) B-X framework becomes unstable, resulting in a two-dimensional (layered) structure. There exists a direct connection between the variable μ and the octahedral structure. When μ is greater than 1, the MX_6 octahedral structure is stable, but when μ is smaller, the structure becomes unstable.

1.6 Why Perovskites Solar Cell ?

Figure 1.14 illustrates the power conversion efficiency of perovskite solar cells (PSCs) in comparison to other technologies. Furthermore, the graph illustrates the gradual growth in power conversion efficiency of technologies other than perovskite solar cells over a span of 50 years, from 1975 to 2024. Perovskite solar cells use these materials as active materials due to their extended charge carrier lifetime, high charge carrier mobility, low exciton binding energy, long diffusion lengths, high open-circuit voltage, and cost-effectiveness.[50] [51][52].

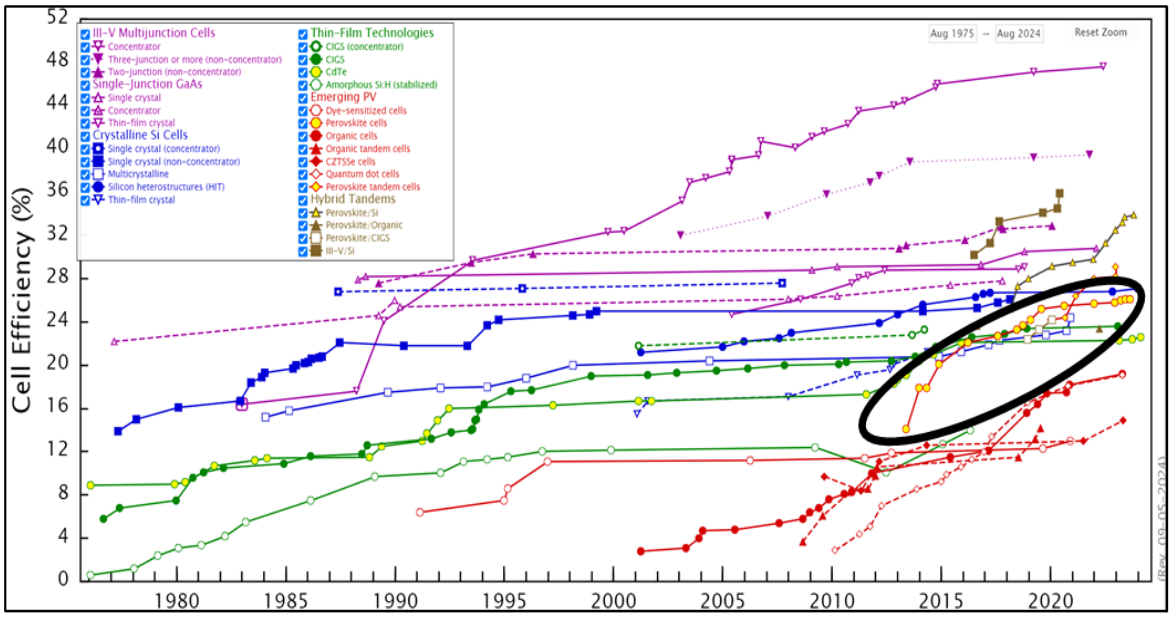

Figure 1.14 Different technology power conversion efficiency trends from 1975 to 2024[53].

As mentioned before, the power conversion efficiency (PCE) of organic-inorganic hybrid perovskite solar cells (PSCs) has been achieved successfully more than 26% in very short span of time (black circle). Nevertheless, there is a concern regarding the degradation of materials and the occurrence of current-voltage hysteresis. Hence, it is imperative to resolve this issue as a prior to the implementation of commercialization. It has been shown that adding Cs atoms to perovskite solar cells makes them more stable and increases their efficiency[54]. As an alternative, the $CsPbX_3$ (where X= Cl, Br, or I) has been taken into consideration due to the fact that it possesses outstanding optoelectronic capabilities and stability[55].

1.7 Litrature Survey on the Perovskite halide solar cell

The journey of the Halide perovskites started in 2005 when they were first used in photovoltaic applications in the Miyasaka laboratory at Toin University in Yokohma, Japan. In 2009, the first peer-reviewed article on Organic-inorganic perovskite-based PV cells was published by

Miyasaka et al. in 2009 [56]. After that, organic–inorganic perovskite solar cells gained a significant amount of attention due to their excellent performance, low-cost fabrication, and flexibility with solutions processing [57][58][59][60][61]. In the last ten years, significant attention has been devoted to perovskite solar cells (PSCs), with a focus on compositional engineering [62][63], investigations on synthesis techniques [64][65], optimization of fabrication methods[66][67][68] and interfacial engineering [69][70]. The certified PCE record of single-junction PSCs has quickly gone from 3.8% at first to as high as 25.7% [56][71][72][73]. This is about the same as the market-leading conventional silicon-based solar cells, which makes it a good candidate for next-generation photovoltaic technology in the near future.

1.7.1 Methyl ammonium Lead Iodide ($MAPbI_3$) Solar Cells

The first Organic-Inorganic perovskite PV cell is based on $MAPbI_3$ ($MA=CH_3NH^+_3$). This perovskite material revolutionized the solar cell efficiency. Initially perovskite based solar cell used $CH_3NH_3PbX_3$ (X = I, Br) as the sensitizer (replacement of dye with perovskite in DSSC solar cell) on a TiO_2 mesoporous electrode. Electrode was utilized in conjunction with an electrolyte solution that contained lithium halide. The solar cell, fabricated utilizing this arrangement, achieved a power conversion efficiency (PCE) that barely reached 3.8%[74]. Instead of low efficiency cell was also show poor stability due to use of a liquid electrolyte. In 2011, Park et al. manufactured liquid dye sensitized solar cells (DSSCs) once again. They used $CH_3NH_3PbI_3$ nanocrystals measuring 2-3 nm, together with an iodide redox shuttle. This resulted in an improved conversion efficiency of the cell, reaching 6.54% under 1 sun light [75]. In both instances, the structure of the perovskite cell was identical, which led to the breakdown of the perovskite material in the liquid electrolyte. As a consequence, the cell

ceased to operate within a few minutes of its construction. So, it was demonstrated that the perovskite material had enormous potential; nevertheless, the cell structure must be altered to make it more stable. In order to identify the solution, two substantial groups collaborated. However, the breakthrough took place in 2012 when Grätzel and his colleagues worked together with Park et al. to examine the use of $MAPbI_3$ in conjunction with the solid hole conductor 2, 20, 7, 7, 0-tetrakis-(N, N-dimethoxyphenylamine)-9, 90-spirobi-fluorene (spiro-MeOTAD) on mesoporous TiO_2 (m-TiO_2), which resulted in an extraordinary PCE of 9.7% [76]. Simultaneously, Snaith and Miyasaka made a breakthrough by developing solar cells using a "meso-superstructured" scaffold. They substituted the n-type mesoporous oxide with an inactive scaffold, specifically Al_2O_3, combined with $CH_3NH_3PbI_{3-x}Cl_x$ and spiro-MeOTAD. This group reported that the cell efficiency was 10.9% [77]. These two studies set the groundwork for the development of perovskite solar cells. Several publications detailing innovative fabrication techniques were published.

Park and Grätzel et al. developed mesoporous TiO_2 and controlled-size $CH_3NH_3PbI_3$ cuboids perovskite solar cells with a best PCE of 17% [78]. Solution-processable perovskite solar cells with the highest efficiency have been produced when an electron collection layer that needs to be sintered at 500 $°C$ is used. This is disadvantageous for cost-effective manufacturing, applications on plastic surfaces, and device topologies with multiple junctions. However, the mechanisms of high efficiency in mesoporous structure-based solar cells are still not fully understood. Next, the planar heterojunction perovskite solar cell was developed through vapour deposition. This cell exhibited a 15.4% PCE, which was equivalent to the 15% efficiency of the mesoporous cell [79]. Consequently, Nicholas and Snaith et al. reported a low-cost, solution-based deposition procedure that employs nanocomposites of graphene and

TiO_2 nanoparticles as the electron collection layers in meso-superstructured perovskite solar cells. These solar cells exhibit exceptional photovoltaic performance, with a power conversion efficiency of up to 15.6% [80]. In 2019, Zhaolai Chen and colleagues successfully created high-efficiency single crystal methyl ammonium lead triiodide (SC-$MAPbI_3$) perovskite solar cells (PSCs) with power conversion efficiencies (PCEs) of 21.09%[81]. In 2020, Lyubov A. Frolova et al. announced that employing polyvinylcarbazole (PVC) as a stabilising agent can drastically reduce photo thermal ageing of $MAPbI_3$.The absorber material's defects are passivated as a result of the PVC addition. Adding the right amount of PVC to $MAPbI_3$ increases the PCE to 18.7% and extends the operational lifetime of solar cells[82]. In 2021, Bekir Turedi published a study on a meticulously cultivated and preserved $MAPbI_3$ single crystal, which had a thickness of 20 μm. By modifying the surface, Single Crystal Sc-PSCs were able to attain an efficiency of 21.93%[83]. Advancements in device performance from materials science and engineering indicate potential for further advancements [84][85][86][87][88]. But the understanding of the mechanisms that are responsible for such outstanding performance has not increased at the same rate as the performance itself.

1.7.2 Formamidinium Lead Iodide ($FAPbI_3$) based solar cells

The substances methylammonium (MA), formamidinium (FA), Cs, and Rb, as well as anions such as I, Br, and Cl, and various combinations of these compounds, have undergone extensive research in recent years.

A site variation:

By varying A site of ABX_3 Perovskite halide we can vary the structural and optical properties of perovskite material. The structural stability achieved by compensating charges within the

PbI_6 octahedra, mostly through electrostatic interactions. Further any change in A-site cation size can shrink or expand the crystal lattice, changing optical characteristics [89].Formamidinium (FA) was the first cation used as replacement of MA in $MAPbI_3$ perovskite material. Since ionic radius of FA^+ (2.53Å) cation is garter than the MA^+(2.17Å) cation thus replacing MA with FA leads better structural stability. Further $FAPbI_3$ ($E_g = 1.47eV$) [90]have lower band gap than $MAPbI_3$ ($E_g = 1.55eV$). Formamidinium lead iodide ($FAPbI_3$) perovskite solar cells show potential because of their absorption edge at 800 nm, which could lead to better performance compared to methyl ammonium lead iodide ($MAPbI_3$). Nevertheless, the actual efficacy of $FAPbI_3$-based cells (~18%) [91] is lower than that of $MAPbI_3$ ($> 20\%$)[92][93][94]. The main issue with $FAPbI_3$ is its phase instability. At room temperature, it crystallises into a photo-inactive yellow phase (δ-$FAPbI_3$), while the photo-active black phase (α-$FAPbI_3$) forms at higher temperatures (125–165℃) and gradually reverts to the yellow phase at RT[62][95].

FA-based perovskites are more susceptible to moisture due to hygroscopic nature of FA. To prevent this, the use of inorganic cations such as caesium (Cs) has been suggested. Incorporating Cs into $MAPbI_3$ ($Cs_{0.09}MA_{0.91}PbI_3$) improves efficiency (up to 18.1%) and thermal stability, retaining performance better during heat treatment than pure $MAPbI_3$[96][52][97]. Similar enhancements are observed when Cs is substituted into $FAPbI_3$[98]. A composition such as $FA_{0.85}Cs_{0.15}PbI_3$ demonstrates improved structural stability and cell performance, even in humid conditions [99].

Further, the stability and efficacy of $FAPbI_3$-based perovskites have been demonstrated to be improved by other alkali metals, such as potassium (K) and rubidium (Rb) [96]. For example,

$Rb_{0.05}FA_{0.95}PbI_3$ perovskites surpass pure $FAPbI_3$ and have superior resistance to moisture depletion. These mixed perovskites show that ion substitution improves perovskite solar cell performance and stability.

X site Variation:

In perovskite solar cells, adding halides (Cl, Br) to lead iodide perovskites like $MAPbI_3$ and $FAPbI_3$, or their mixed-cation versions, affects optical and electrical properties like band gap, carrier lifetime, and diffusion length. The X-site halides have a far more significant impact on the material's performance than the A-site cations.

Despite some controversy, it has been reported that adding chloride (Cl) to $MAPbI_3$ improves film quality. This is because it slows down crystallization, resulting in films that are more uniform and absence of pinholes. As a result, the device's performance and stability are both enhanced. However, Cl sublimates during film formation, making its presence in the perovskite film questionable. However, adding Cl-based additives such as $PbCl_2$, HCl, NH_4Cl, and MACl can enhance crystallinity and electron diffusion length, indirectly boosting cell efficiency [100][101][102][103][104][105][106].

Incorporating bromide (Br) has a more noticeable and immediate effect. The band gap (E_g) of $MAPbI_3$ grows quadratic with Br concentration when Br is mixed in. This tuning optimises perovskite characteristics for specific applications. Early research found efficiency of over 12% with less than 10% Br, later work using improved preparation techniques led to increases of up to 16.2%. Perovskites that contain Br- also have better resistance to humidity. This is because their structures change from tetragonal to pseudo cubic phases [107][108].Similarly, the band gap is increased by Br incorporation in $FAPbI_3$-based perovskites, although an

amorphous phase is formed when the Br content is excessive ($x > 2.3$), the source of which is not completely known [109].

1.7.3 Mixed perovskite halide

Photovoltaic (PV) systems have seen a major advancement with the emergence of mixed cation and halide perovskites, which has improved cell stability and efficiency significantly. Perovskites have been the subject of substantial research into improving their optoelectronic characteristics by optimising their composition with a variety of cations and mixed halides, including caesium (Cs), formamidinium (FA), and methylammonium (MA).

FA-MA Mixed Perovskites: By incorporating MA into $FAPbI_3$ perovskite, the Goldschmidt tolerance factor is adjusted, which in turn stabilises the cubic phase of the perovskite. The process of mixing different elements has demonstrated enhanced device functionality and durability. The composition $MA_{0.17}FA_{0.83}Pb(I_{0.83}Br_{0.17})_3$ has demonstrated power conversion efficiencies (PCE) more than 20%. Additional improvements have been found by using a novel hole transport material (HTM). Nevertheless, the persistence of the photo-inactive yellow phase poses a difficulty for maintaining long-term stability[110][111].

Role of Cs, Rb, and K in Mixed Perovskites: There are distinct functions that Cs and Rb fulfil inside perovskite structures. Cs, which can enter the crystal lattice, lowers trap states, increasing V_{oc} and FF. Conversely, Rb separates and decreases surface recombination. When Cs and Rb work together, they produce perovskites that are more charge carrier mobile and have fewer traps, which improves their performance[112][113]. K^+ which is about the same size as Rb, has been shown to "passivate" defect sites in perovskites. This lowers hysteresis in J-V curves and makes the cell work better overall. K^+ does not occupy crystal sites in

perovskite, but it prevents the formation of the photo inactive δ-phase and increases charge carrier lifespan and recombination rates [114][115][116].

Challenges and Future scope: Although progress has been made, the methods by which these cations improve perovskite performance remain unknown. Additional research is needed to address questions such as how various cations contribute to defect passivation, how ions are distributed throughout the perovskite layer, and what impact changes to the surface composition have specifically. recognising these variables will be essential in creating perovskites with enhanced efficiency and stability.In conclusion, combined cation and halide perovskites have advanced perovskite solar cell technology. Cs, Rb, and K have improved structural stability, defect passivation, and device performance, advancing the search for high-efficiency, stable perovskite solar cells[117][118].

1.7.4 Inorganic solar cells

Organic-inorganic hybrid perovskites, such as $MAPbI_3$ and $FAPbI_3$, exhibit excellent efficiency but lack long-term stability due to the inclusion of organic cations, such as methylammonium (MA) and formamidinium (FA). These materials undergo degradation at relatively low temperatures, with $MAPbI_3$ undergoing decomposition at approximately 120℃ or even as low as 80℃ over prolonged durations. One possible solution to this problem is to increase stability by substituting inorganic cations, such as caesium (Cs^+), for organic ones. Caesium-based perovskites, namely $CsPbX_3$ (X = Cl, Br, I), exhibit enhanced thermal stability and have been the subject of research since the 1980s [119]. Although $CsPbI_3$ perovskite solar cells (PSCs) initially encountered difficulties, recent studies have resulted in substantial enhancements in their power conversion efficiency (PCE), rising from 2.9% in 2015 to 15.7%

in recent research [120][121]. This demonstrates the promising prospects of utilising all-inorganic perovskites in solar energy applications.

Black phase of $CsPbI_3$:

$CsPbI_3$ encounters substantial challenges in maintaining its black photoactive phase (α-$CsPbI_3$) at room temperature (RT). It usually forms a yellow phase (δ-$CsPbI_3$) at RT, while the black phase remains stable only at temperatures above 310 $°C$ [120]. The reason for this is the limited size of the Cs^+ cation, which is not enough to maintain the cubic structure at lower temperatures. In order to stabilise α-$CsPbI_3$, researchers have investigated the possibility of increasing the tolerance factor by partially substituting Cs^+ with larger cations (such as MA^+ and FA^+) or I^- with smaller anions (such as Br^- and Cl^-) [122].

Despite the progresses, there are still many problems to solve. The precise mechanisms of stabilisation and the consequences of charge neutrality on electronic characteristics are not fully understood. Recent investigations demonstrate that massive crystal grains can stabilise the black phase with PCEs up to 17 % [121][123]. To fully realise the promise of $CsPbI_3$-based perovskite solar cells, more investigation is required to better understand the crystallisation process and degradation mechanisms, find appropriate dopants, and optimise annealing settings.

Cesium−Lead Mixed Halide Perovskites:

$CsPbBr_3$, with a band gap of ~ 2.3 eV, is less suitable for PV applications but has superior thermal stability up to 580 $°C$, unlike $MAPbBr_3$, which degrades at 220 $°C$. The photoactive phase of $CsPbBr_3$ is stable at room temperature (RT), which enables its utilisation in perovskite solar cells (PSCs) with efficiencies of approximately 6 % [124]. The thermal stability of

$CsPbBr_3$ and the smaller band gap of $CsPbI_3$ have been combined to create mixed halide perovskites ($CsPbI_{3-x}Br_x$). These enable fine control of the band gap by adjusting the I/Br ratio, with $CsPbI_2Br$ obtaining a band gap of 1.9 eV and a power conversion efficiency (PCE) of 13.3 % via a two-step annealing process [125]. $CsPbI_2Br$ also exhibits greater stability than inorganic-organic PSCs, shedding just 20 % of its original PCE after 360 hours at 85 $°C$ [126].

1.7.5 Lead free perovskite solar cell

Despite perovskite solar cells' (PSCs) effectiveness, lead toxicity prevents their commercialisation. Lead is one of the top 10 most hazardous elements, affecting many physiological systems [127]. Although lead in PSCs has a poor solubility and is unlikely to spread, environmental concerns remain. This has prompted study into decreasing or removing lead in perovskites, with safer alternatives and mitigating measures being investigated to reduce the impact [128][129].

Tin (Sn)-based perovskites are becoming more popular as lead-free options because they have similar ionic radii to lead (Pb) and better optoelectronic qualities than Pb-based perovskites, such as lower band gaps and higher charge carrier mobilities [130][131]. However, difficulties like oxidation of Sn^{2+} to Sn^{4+} and poor film quality limit their efficiency in solar cells.

To solve these challenges, numerous techniques have been implemented. The use of SnF_2 has showed promise in lowering background carrier density and avoiding oxidation, resulting to increased performance up to 2.1 % [132]. Experiments with cations and additives like hydrazine or $SnCl_2$ have improved stability and efficiency. For instance, a two-step deposition method produced stable, high-quality films, and $SnCl_2$ enhanced stability and served as an electron transport layer [133][134]. One recent development is the addition of

phenylethylammonium (PEA) to $FASnI_3$, which improves stability and achieves efficiencies of up to 9% [135]. Despite these advancements, Sn perovskites perform worse than Pb perovskites due to oxidation, film quality difficulties, and interfacial layer sensitivity. To further improve the stability and efficacy of Sn-based perovskites, it is imperative to conduct additional research on charge transport layers, cation mixing, and additives [136][137].

1.8 Issues with the Perovskite Halides Solar Cell

Perovskite solar cells possess immense potential for the future of sustainable energy. However, there exist several significant challenges that scientists and engineers must overcome prior to their commercial production. The challenges mentioned have an impact on various aspects of perovskite solar cell technology, including its stability, Hysteresis, scalability, toxicity, and production processes[138].

1.8.1 Stability Issues with Perovskites

To commercialise perovskite solar cells (PSCs), long-term stability and lead toxicity must be addressed. Although laboratory-scale devices can achieve power conversion efficiencies (PCE) of over 20%, photovoltaic solar cells (PSCs) need to exhibit consistent power generation for a period of around 25 years in real-world conditions, which include exposure to sunlight, high temperatures, humidity, and oxygen. Preventing performance and material degradation requires intrinsic stability and environmental stress resistance, which must be addressed immediately for commercialisation.

1.8.1.1 Structural/Intrinsic Stability

The Goldschmidt tolerance factor (τ) affects perovskite compound stability, with optimal stability occurring between 0.8 and 1. Mixed perovskites, which involve the combination of various cations and anions, enhance stability but may encounter challenges such as the development of non-perovskite phases and degradation caused by strain [139]. A significant obstacle is the migration of ions, especially iodide and MA^+ ions, which is facilitated by crystal defects and grain boundaries [140][141][142]. There are additional factors that influence stability, including stress-induced phase transitions, thermal strain, and crystal orientation [143][144]. To improve perovskite stability, strategies like as compositional engineering and stress control are essential [145].

1.8.1.2 External/Environmental Stability

Long-term performance requires perovskite stability in moisture, oxygen, and light. Reversible hydration can occur with just a little moisture, but irreversible deterioration can occur with an excess of water. One way to tackle this is via encapsulating or by making surface alterations that are hydrophobic. Stability is also influenced by oxygen and light exposure. Oxygen causes degradation, while light induces photo-instability, phase segregation, and ion migration [146][147][148]. Stability has been improved with 2D/3D perovskite mixtures, hydrophobic polymers, and alternate electron transport layers [149]. Encapsulation and UV-resistant coatings are two techniques used to reduce these impacts and increase the durability of perovskite solar cells [150].

1.9 Current –Voltage(J-V) Hysteresis

Even though Perovskite solar cells (PSCs) are a popular choice for next-generation PV technology due to their low cost production and High power conversion efficiency (PCE). Perovskite solar cells (PSCs) achieved a remarkable power conversion efficiency (PCE) of 26.1% in 2024, approaching the level of efficiency exhibited by the currently available extremely efficient crystalline silicon (Si) solar cells. Perovskite materials are photoactive substances with a direct bandgap, which leads to a greater ability to absorb light in the visible spectrum compared to silicon. They can also better tune their bandgap, which ranges from 1.4 eV to 2.3 eV. Perovskite materials exhibit a high dispersion of the conduction band and valence band, allowing for efficient electron and hole transport and reducing the recombination of photo generated charge carriers.The exceptional characteristics of perovskite materials make them a highly desirable option for replacing silicon solar cells, which currently hold a dominant position in the market. The hysteresis problem in perovskites was initially observed in 2014 [138][151]. J-V hysteresis, however, is a common problem in PSCs and has a significant impact on device performance[35]. Consequently, it is essential to determine the cause of the hysteresis in PSCs and develop suitable remedies to deal with it. The hysteresis index quantifies the severity of hysteresis:

$$\text{HI}=(PCE_{RS}\text{-}PCE_{FS})/PCE_{RS} \quad (1.8)$$

The power conversion efficiencies for the reverse scan (RS) and forward scan (FS) are represented by PCE_{RS} and PCE_{FS}, respectively. Hysteresis has been observed in numerous dissipative devices and systems. [152]. Hysteretic behaviour is commonly found in systems

that demonstrate a delay in the changing of their properties in response to external stimuli, such as electrical and optical fields.

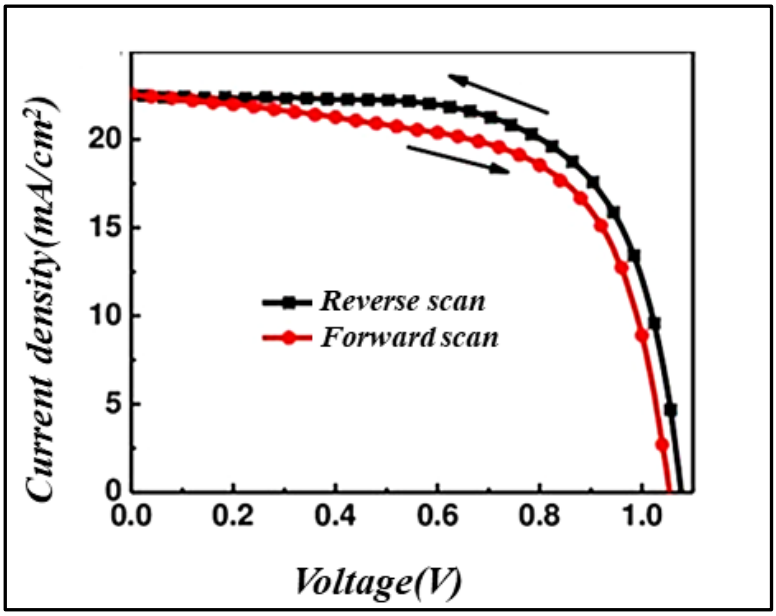

Figure 1.15 Current-Voltage hysteresis in PSC [153].

The figure (1.15) show the properties of the current-voltage (J-V) relationship in forward scan (FS) and reverse scan (RS) scenarios. An observable disparity in J values occurs as V increases between FS and RS , referred to as J-V hysteresis.Numerous investigations, including those conducted by [154], [155] and [156] have identified numerous causes of hysteresis in PSCs. Some of these reasons are: (i) due to the fact that the photoactive perovskite material possesses a ferroelectric feature (ii) The choice and morphology of the transport layers (compact or mesoporous) are critical factors in determining the imbalanced transport of charge carriers, which is influenced by the hole transport layers (HTLs) and electron transport layers (ETLs) (iii) migration of ions; and (iv) The process of trapping/detrapping of charge carriers.[157] found that hysteresis in PSCs is influenced by external scanning factors, including rate, electric

field, direction, and pre-scanning circumstances. One of the obstacles that prevents PSCs from being commercialised is the peculiar hysteretic conduct that they exhibit.

1.10 Motivation

According to the literature review, perovskite halide materials used for solar cell fabrication have excellent properties such as extended charge carrier lifetime, high charge carrier mobility, low exciton binding energy, long diffusion lengths, high open-circuit voltage, and cost-effectiveness. Furthermore, perovskite-based solar cells have very high efficiency. However, before commercialization, we must resolve several problems associated with the perovskite-based solar cell. One such problem is hysteresis in the perovskite-based solar cell, which significantly impacts its efficiency. The precise cause of this hysteresis remains unknown. This is the motivation behind my work to investigate the origin of J-V hysteresis and the effect of polarization on inorganic perovskite halides such as $CuPbI_3$, $CuSnI_3$, and $CsSnI_3$.

1.11 The Objective Of Current Research

This chapter addresses the major issue of I-V hysteresis in perovskite halides. The primary goal of this study is to determine the reason of hysteresis in the current-voltage (I-V) properties of perovskite halides. In order to industrialise photovoltaic applications, it is essential to have a thorough understanding of the problem of current-voltage hysteresis, which must be resolved before industrialisation. For this purpose, Inorganic perovskite $CuPbI_3$, $CuSnI_3$, and $CsSnI_3$ have been selected as active materials.

The major work plan of this thesis is discussed below:

1. The grain-grain boundary interface in polycrystalline halides, like ferroelectric materials, significantly impacts hysteresis behaviour by changing polarisation mechanisms, which remains unexplored. To achieve this goal, we synthesized new material, such as $CuPbI_3$, which have excellent conductivity. These materials were used to investigate their potential applications in photoconductive systems.Compared to $CsPbI_3$ and $CsPbBr_3$, $CuPbI_3$ is a lesser-known material with ambiguous structural properties.
2. After exploring $CuPbI_3$, we replaced Pb with Sn and altered the polarization mechanism by dpoling. We then studied the effect of poling and temperature on the current-voltage hysteresis in lead-free perovskite halide $CuSnI_3$.
3. We replaced Cu with Cs in $CuSnI_3$ and observed the impact of temperature and DC polarization on the hysteresis area of the current-voltage (IV) curve caused by the photo-field in the lead-free $CsSnI_3$.

1.12 Plan of the Present Thesis

The work in this thesis is structured into six chapters and a brief description of each of the chapters is as follows:

Chapter 1: This chapter provides an overview of solar cells, including comprehensive reviews of existing literature. It presents an analysis of the factors that drive work motivation, the historical context, and the basic principles of solar cells. It also highlights the necessary characteristics of active materials for perovskite solar cells. Furthermore, literature studies have identified major challenges in perovskite halides (active materials). The chapter describes the current-voltage hysteresis problem in perovskite solar cells. This chapter also addresses the primary goals of the current study.

Chapter 2: This chapter explains the various experimental methods used in the current study. It describes the experimental equipment, analysis procedures, and synthesis routes used to produce the samples. The suggested system was synthesized using cold sintering procedures via a solid-state reaction process. It also provides a comprehensive overview of critical analytical techniques, including Rietveld refinement analysis. Additionally, it provides a detailed description of a variety of instruments, including XRD, SEM, TGA, DSC, UV-visible, AFM/PFM, DC Poling Unit, Electrometer for Pyro-current Measurement, Raman, impedance spectroscopy, and I-V measurement.

Chapter 3: Aim of this chapter to investigate the change in polarisation behaviour at the surface/interface of $CuPbI_3$ before and after light exposure. By altering the polarisation mechanism by varying the sintering temperature, compound $CuPbI_3$ was synthesised through the cold sintering technique. We also predicted the structure of $CuPbI_3$. Further, the chapter will explore the effects of light exposure on $CuPbI_3$ hysteresis area and shape, impedance analysis, and conduction/hopping mechanisms**.**

Chapter 4: Due to environmental concerns and lead toxicity, there has been significant interest in the development of lead-free alternatives. Lead-free perovskite halides, such as tin-based (Sn) perovskites. This chapter investigate the photo hysteresis behaviour and the impact of phase transitions on the hysteresis of the lesser known lead free compound $CuSnI_3$. Lead free halides perovskite $CuSnI_3$ was synthesized by the cold sintering method. Further to investigate the impact of potential phase transitions on current voltage hysteresis, we examined the temperature-dependent behaviour of the current voltage curve in both dark and light conditions, specifically in the presence of probable anomalies or phase transitions, such as AM 1.5 G. To observe the inherent characteristics of these irregularities, we subjected the sample

to an electric field of 0.5 kV for a duration of 30 minutes. We then compared the current voltage behaviour of the sample with its original state at a temperature of 300 K under normal environmental conditions.

Chapter 5: This chapter describes the isomorphic phase transition in the green polymorph of $CsSnI_3$ (G-$CsSnI_3$), which is cubic ($Pa\bar{3}$) at 295 K and persists phase transitions at higher temperatures. We used PFM, temperature-dependent dielectric measurements, impedance spectroscopy, and Raman spectroscopy. To investigate the impact of the phase transition on current voltage hysteresis, we examined the temperature-dependent behaviour of the current voltage curve under dark and light conditions (AM 1.5 G) around the phase transition. The poling impacts both domain size and grain number. Light and poling both appear to affect the relaxation time, which changes over transitions.

Chapter 6: This chapter concludes the findings of this research outcome and lists a few possibilities for future investigations.